The optical nonreciprocal response based on a four-mode optomechanical system

Jing Wang(王婧)†

College of Physics, Tonghua Normal University, Tonghua 134000, *China*

(Received 4 September 2019; revised manuscript received 20 November 2019; accepted manuscript online 7 January 2020)

We propose a scheme for realizing the optical nonreciprocal response based a four-mode optomechanical system, consisting of two charged mechanical modes and two linearly coupled optical modes. Two charged mechanical modes are coupled by Coulomb interaction, and two optical modes are coupled to one of mechanical modes by radiation pressure. We numerically evaluate the transmission probability of the probe field to obtain the optimum optical nonreciprocal response parameters. Also, we show that the optical nonreciprocal response is caused by the quantum interference between the optomechanical couplings and the linearly coupled interaction that breaks the time-reversal symmetry.

Keywords: optical nonreciprocal response, optomechanical system, phase difference

PACS: 42.50.–p, 42.50.Wk **DOI:** 10.1088/1674-1056/ab6836

1. Introduction

Cavity optomechanical systems have attracted a great deal of attention from both theorists and experimentalists in recent years.[1–36] The systems demonstrate the interaction between the movable mechanical resonator and the optical field in the cavity by radiation pressure, and becomes a platform for studying optomechanically induced transparency (OMIT),[2–12] optomechanically induced amplification,[13,14] ground-state cooling of the mechanical resonator,[15–18] normal-mode splitting,[19] parity-time-symmetry-breaking chaos,[20] and so on. Recently, OMIT has been studied in various cavity optomechanical systems.[6–12] For example, Zhang *et al.* proposed a potentially practical scheme to precisely measure the charge number of small charged objects using OMIT in an optomechanical system, where the charged mechanical mode is subject to the Coulomb force due to the charged body nearby.[34] Wu investigated the properties of the tunable ponderomotive squeezing by Coulomb interaction in a cavity optomechanical system.[22]

In the past decades, a phenomenon called nonreciprocity effect has been predicted theoretically and observed experimentally.[37–41] The nonreciprocity effect is the basis of directional amplifiers, isolators, circulators,[37] and an important device for information processing. This effect is usually caused by breaking the time-reversal symmetry of photons. There are four main ways to break the time-reversal symmetry of photons: (i) using magneto-optical effects,[37] (ii) using non-magnetic strategies of optical nonlinearity,[38,39] (iii) using dynamic modulation,[40] and (iv) using angular momentum biasing.[41] Recently, it is noteworthy that some researchers have used the radiation-pressure-induced optomechanical coupling to break the time-reversal symmetry and to realize the nonreciprocal effects for light.[42–56] The significant achievements have been made in this field, including nonreciprocal amplification,[42] nonreciprocal transmission,[43,44] nonreciprocal single-photon effects,[45] and nonreciprocal slow light,[9,47] etc. Jiang *et al.* proposed a scheme for realizing optical directional amplification between optical and microwave fields based on an optomechanical system with optical gain.[48] They found that the direction of amplification can be controlled by the phase differences between the effective optomechanical couplings. Xu *et al.* showed the optical nonreciprocal response in a three-mode optomechanical system consisting of two optical modes and one mechanical mode.[53] They proved that the optical nonreciprocal response is achieved by adjusting the phase difference between the optomechanical coupling rates to cause breaking of time-reversal symmetry of the system. Xu *et al.* demonstrated the possibility of a three-port circulator in a three-mode optomechanical system, which is referred to as an optomechanical circulator.[51] Li *et al.* studied a three-mode optomechanical system, where the mechanical mode is subject to the additional mechanical drive.[46] When the driving frequency of the mechanical mode is equal to the frequency difference between the optical probe and pump fields, the system will get directional amplification of an optical probe field.

Inspired by Ref. [48], we naturally ask whether the optical nonreciprocity can be realized by Coulomb interaction in optomechanical system or not. If possible, what are new insights that the Coulomb interaction will bring about for the optical nonreciprocal response? Based on the above problems, we theoretically study how to realize the optical nonreciprocal response based on a four-mode optomechanical system. As shown in Fig. 1, two charged mechanical mode are coupled by

†Corresponding author. E-mail: pwl1207wj@163.com

Coulomb interaction. One mechanical mode is coupled with two directly coupled optical modes respectively. In addition, two optical modes are driven by two coupling fields respectively. The optical nonreciprocal response can be achieved when the four-mode optomechanical system works under certain conditions. We will also clarify the role of each physical quantity in the system. The main differences between our work and Ref. [48] are: (1) The systems that form the optical nonreciprocal response are different. The system in Ref. [48] consists of two optical modes and one mechanical mode. The system we consider contains two optical modes and two charged mechanical modes coupled by Coulomb interaction. As far as optomechanically induced transparency is considered, there have been schemes utilizing charged objects in cavity optomechanical systems.[22,33,34] However, no proposals have been found to combine both mechanical modes and Coulomb interaction for studying the optical nonreciprocal response in quantum optomechanics though much richer nonlinear phenomena are expected. (2) We will discuss the optimal parameters of observing the optical nonreciprocal response. Furthermore, Compared with Refs. [46,51], there is no additional mechanical drive in the mechanical mode of our system, so our system is more stable.

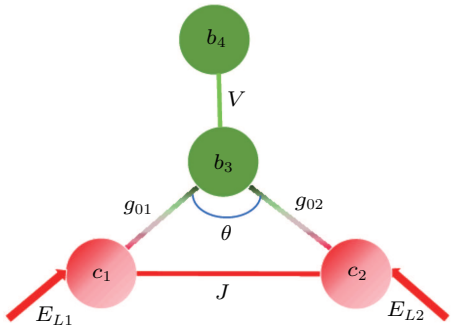

Fig. 1. The schematic of the four-mode cavity optomechanical system consisting of two optical modes (c_1 and c_2) and two charged mechanical modes (b_3 and b_4). The optical modes and the mechanical mode b_3 are coupled via radiation pressure. The mechanical modes b_3 and b_4 are coupled via Coulomb interaction.

The paper is organized as follows. In Section 2, we introduce the theoretical model, the detailed analytical expressions of the optomechanical system, and obtain the transmission probability of the probe field. In Section 3, we discuss in detail the effect of the phase difference, the Coulomb coupling, and the effective optomechanical coupling strengths on the optical nonreciprocal response. Finally, in Section 4, we summarize our work.

2. Model and equations

The four-mode optomechanical system under consideration is schematically shown in Fig. 1, including two optical modes (c_i, frequency ω_{ci}, length L_i $(i=1,2)$) and two charged mechanical modes (b_j, effective mass m_j, frequency ω_{mj} and damping rate γ_{mj} $(j=3,4)$). Two optical modes couple directly with coupling strength J. Furthermore, the two optical modes couple with the charged mechanical mode b_3 respectively, and the optomechanical coupling strength is $g_{0i}=\sqrt{1/2m_3\omega_{m3}}\omega_{ci}/L_i$ $(i=1,2)$. The charged mechanical mode b_3 is coupled to the other charged mechanical mode b_4 by a tunable Coulomb interaction V. The b_3 and b_4 take the charges $Q_3=C_3V_3$ and $Q_4=C_4V_4$, with C_3 (C_4) and V_3 (V_4) being the capacitance and the voltage of the bias gate,[22] respectively. The two optical modes are driven by the strong coupling field $E_{Li}=\sqrt{2P_i\kappa_i/\omega_{Li}}$ with frequency $\omega_{Li}=2\pi c/\lambda_i$ (λ_i $(i=1,2)$ represents the wavelength, c is the speed of light in vacuum), in which P_i $(i=1,2)$ denotes its power and κ_i is the total damping rate of optical mode c_i $(i=1,2)$. Without loss of generality, here we have assumed that J, g_{0i}, V and E_{Li} $(i=1,2)$ are real numbers. The Hamiltonian of the four-mode optomechanical system is ($\hbar=1$)

$$\begin{aligned} H &= \sum_{i=1,2}\omega_{ci}c_i^\dagger c_i+\sum_{j=3,4}\omega_{mj}b_j^\dagger b_j \\ &\quad+\sum_{i=1,2}g_{0i}c_i^\dagger c_i(b_3^\dagger+b_3)\cos(\theta/2) \\ &\quad+J(c_1^\dagger c_2+c_2^\dagger c_1)+V(b_3^\dagger b_4+b_4^\dagger b_3) \\ &\quad+\sum_{i=1,2}i(E_{Li}c_i^\dagger \mathrm{e}^{-\mathrm{i}\omega_{Li}t}-E_{Li}^\dagger c_i \mathrm{e}^{\mathrm{i}\omega_{Li}t}), \end{aligned} \tag{1}$$

where the first and second terms denote the free energies of two optical modes and two mechanical modes, respectively, the $c_i^\dagger$ (c_i) is the creation (annihilation) operator of the optical mode c_i satisfying the commutation relation $[c_i,c_i^\dagger]=1$ $(i=1,2)$, $b_j^\dagger$ (b_j) is the creation (annihilation) operator of the mechanical mode b_j satisfying the commutation relation $[b_j,b_j^\dagger]=1$ $(j=3,4)$. The third term denotes the nonlinear optomechanical interactions between the two optical modes and mechanical mode b_3, and θ is the angle between the incident light and the reflected light at the surfaces of the mechanical mode b_3. The fourth term describes the interaction between the c_1 and c_2. The Coulomb interaction between the b_3 and b_4 is given by the fifth term. The last term gives the interaction of the optical modes with the strong coupling fields. In a frame rotating at the $H_{\rm rotating}=\sum_{i=1,2}\omega_{ci}c_i^\dagger c_i+\sum_{j=3,4}\omega_{mj}b_j^\dagger b_j$ and neglecting the counterrotating and higher-order terms with $|c_i|\gg 1$ $(i=1,2)$, the Hamiltonian of the whole system takes the form

$$\begin{aligned} H_{\rm rotating} &= G_1(c_1b_3^\dagger \mathrm{e}^{\mathrm{i}\phi_1}+c_1^\dagger b_3\mathrm{e}^{-\mathrm{i}\phi_1})\cos(\theta/2) \\ &\quad+G_2(c_2b_3^\dagger \mathrm{e}^{\mathrm{i}\phi_2}+c_2^\dagger b_3\mathrm{e}^{-\mathrm{i}\phi_2})\cos(\theta/2) \\ &\quad+J(c_1^\dagger c_2+c_2^\dagger c_1)+V(b_4^\dagger b_3+b_3^\dagger b_4). \end{aligned} \tag{2}$$

Here we have set $\omega_{Li}-\omega_{ci}=-\omega_{m3}$ (red sideband) and $g_{0i}c_i=g_{0i}|c_i|\,\mathrm{e}^{\mathrm{i}\phi_i}=G_i\mathrm{e}^{\mathrm{i}\phi_i}$ with G_i being the effective optomechanical coupling strengths between the mechanical mode b_3 and optical mode c_i $(i=1,2)$. The phases $\phi_i\,(i=1,2)$ can be absorbed by redefining the operators c_i, and only the phase

difference $\phi = \phi_2 - \phi_1$ has physical effects.[48] Consequently, equation (2) becomes

$$\begin{aligned} H_{\text{rotating}} &= G_1(c_1 b_3^\dagger + c_1^\dagger b_3)\cos\theta/2 \\ &\quad + G_2(c_2 b_3^\dagger \mathrm{e}^{\mathrm{i}\phi} + c_2^\dagger b_3 \mathrm{e}^{-\mathrm{i}\phi})\cos(\theta/2) \\ &\quad + J(c_1^\dagger c_2 + c_2^\dagger c_1) + V(b_4^\dagger b_3 + b_3^\dagger b_4). \end{aligned} \tag{3}$$

In Eq. (3), interaction of "beam-splitter", such as $G_1(c_1 b_3^\dagger + c_1^\dagger b_3)\cos(\theta/2)$ or $G_2(c_2 b_3^\dagger \mathrm{e}^{\mathrm{i}\phi} + c_2^\dagger b_3 \mathrm{e}^{-\mathrm{i}\phi})\cos(\theta/2)$, leads to optomechanically induced transparency and quantum state transfer.[50]

Starting from the Heisenberg equation of motion $\mathrm{i}\dot{\hat{O}} = \left[\hat{O}, \hat{H}\right]$, taking into account the dissipations of the optical modes and the mechanical modes, and adding quantum noise and thermal noise, we can give the time evolutions of the expectation values of the system operators as follows:

$$\begin{aligned} \dot{c}_1 &= -\frac{\kappa_1}{2}c_1 - \mathrm{i}G_1 b_3 \cos\frac{\theta}{2} - \mathrm{i}Jc_2 \\ &\quad + \sqrt{\kappa_{\text{ex1}}}c_{\text{in1}}(t) + \sqrt{\kappa_{01}}c_{\text{in1}}^0(t), \\ \dot{c}_2 &= -\frac{\kappa_2}{2}c_2 - \mathrm{i}G_2 b_3 \mathrm{e}^{-\mathrm{i}\phi}\cos\frac{\theta}{2} - \mathrm{i}Jc_1 \\ &\quad + \sqrt{\kappa_{\text{ex2}}}c_{\text{in2}}(t) + \sqrt{\kappa_{02}}c_{\text{in2}}^0(t), \\ \dot{b}_3 &= -\frac{\gamma_{m3}}{2}b_3 - \mathrm{i}G_1 c_1 \cos\frac{\theta}{2} - \mathrm{i}G_2 c_2 \mathrm{e}^{\mathrm{i}\phi}\cos\frac{\theta}{2} \\ &\quad - \mathrm{i}Vb_4 + \sqrt{\gamma_{m3}}b_{\text{in3}}(t), \\ \dot{b}_4 &= -\frac{\gamma_{m4}}{2}b_4 - \mathrm{i}Vb_3 + \sqrt{\gamma_{m4}}b_{\text{in4}}(t), \end{aligned} \tag{4}$$

with $\kappa_i = \kappa_{\text{ex}i} + \kappa_{0i}$, where $\kappa_{\text{ex}i}$ and κ_{0i} $(i = 1,2)$ are the external coupling rate and the intrinsic dissipation rates, respectively.[48] Equation (4) can be cast into a matrix form

$$\dot{u}(t) = Au(t) + Lu_{\text{in}}(t), \tag{5}$$

where the two column vectors are

$$\begin{aligned} &u(t) = (c_1, c_2, b_3, b_4)^{\mathrm{T}}, \\ &u_{\text{in}} = (c_{\text{in1}}(t), c_{\text{in2}}(t), c_{\text{in1}}^0(t), c_{\text{in2}}^0(t), b_{\text{in3}}(t), b_{\text{in4}}(t))^{\mathrm{T}}. \end{aligned} \tag{6}$$

The damping matrix is given by

$$L = \begin{pmatrix} \sqrt{\kappa_{\text{ex1}}} & 0 & \sqrt{\kappa_{01}} & 0 & 0 & 0 \\ 0 & \sqrt{\kappa_{\text{ex2}}} & 0 & \sqrt{\kappa_{02}} & 0 & 0 \\ 0 & 0 & 0 & 0 & \sqrt{\gamma_{m3}} & 0 \\ 0 & 0 & 0 & 0 & 0 & \sqrt{\gamma_{m4}} \end{pmatrix}, \tag{7}$$

and the coefficient matrix A is given by

$$A = \begin{pmatrix} \frac{-\kappa_1}{2} & -\mathrm{i}J & -\mathrm{i}G_1\cos\frac{\theta}{2} & 0 \\ -\mathrm{i}J & \frac{-\kappa_2}{2} & -\mathrm{i}G_2\mathrm{e}^{-\mathrm{i}\phi}\cos\frac{\theta}{2} & 0 \\ -\mathrm{i}G_1\cos\frac{\theta}{2} & -\mathrm{i}G_2\mathrm{e}^{\mathrm{i}\phi}\cos\frac{\theta}{2} & \frac{-\gamma_{m3}}{2} & -\mathrm{i}V \\ 0 & 0 & -\mathrm{i}V & \frac{-\gamma_{m4}}{2} \end{pmatrix}. \tag{8}$$

The stability conditions of the system require all the real parts of the eigenvalues of matrix A to be negative, which can be analyzed by the Routh–Hurwitz criterion.[57,58] The pushing process is too complicated, so we omitted it here.

The Fourier transform of the operators are given by

$$\begin{aligned} f(\omega) &= \frac{1}{\sqrt{2\pi}}\int_{-\infty}^{+\infty} \mathrm{e}^{\mathrm{i}\omega t} f(t)\,\mathrm{d}t, \\ f(t) &= \frac{1}{\sqrt{2\pi}}\int_{-\infty}^{+\infty} \mathrm{e}^{-\mathrm{i}\omega t} f(\omega)\,\mathrm{d}\omega. \end{aligned} \tag{9}$$

According to Eq. (9) and using the properties of Fourier transformation, the solution to Eq. (5) in the frequency domain is

$$u(\omega) = -(A + \mathrm{i}\omega I)^{-1} L u_{\text{in}}(\omega), \tag{10}$$

where I denotes the identity matrix.

The input-output theorem is[2]

$$u_{\text{out}}(\omega) = u_{\text{in}}(\omega) - L^{\mathrm{T}} u(\omega). \tag{11}$$

Substituting Eq. (10) into Eq. (11), we can obtain

$$u_{\text{out}}(\omega) = T(\omega) u_{\text{in}}(\omega), \tag{12}$$

where the output field vector $u_{\text{out}}(\omega)$ is the Fourier transform of

$$u_{\text{out}} = (c_{\text{out1}}, c_{\text{out2}}, c_{\text{out1}}^0, c_{\text{out2}}^0, b_{\text{out3}}, b_{\text{out4}})^{\mathrm{T}}, \tag{13}$$

and the transmission matrix is given by

$$T(\omega) = I + L^{\mathrm{T}}(A + \mathrm{i}\omega I)^{-1} L. \tag{14}$$

Here the matrix element $T_{ij}(\omega)$ represents the transmission probability of the probe field from cavity c_j to cavity c_i $(i, j = 1,2)$. We can obtain the transmission matrix elements T_{12} and T_{21} as

$$\begin{aligned} |T_{12}| &= \frac{\sqrt{\kappa_{\text{ex1}}}\sqrt{\kappa_{\text{ex2}}}(\mathrm{i}V^2 J - A_4(-\mathrm{i}JA_3 + G_1 G_2 \cos^2\frac{\theta}{2}\mathrm{e}^{\mathrm{i}\phi}))}{V^2(J^2 - A_1A_2) + A_4[A_3(J^2 - A_1A_2) + \mathrm{i}\cos^2\frac{\theta}{2}(G_1^2A_2 + 2G_1G_2J\cos\phi + G_2^2A_1)]}, \\ |T_{21}| &= \frac{\sqrt{\kappa_{\text{ex1}}}\sqrt{\kappa_{\text{ex2}}}(\mathrm{i}V^2 J - A_4(-\mathrm{i}JA_3 + G_1 G_2 \cos^2\frac{\theta}{2}\mathrm{e}^{-\mathrm{i}\phi}))}{V^2(J^2 - A_1A_2) + A_4[A_3(J^2 - A_1A_2) + \mathrm{i}\cos^2\frac{\theta}{2}(G_1^2A_2 + 2G_1G_2J\cos\phi + G_2^2A_1)]}, \end{aligned} \tag{15}$$

where $A_1 = i\kappa_1/2 + \omega$, $A_2 = i\kappa_2/2 + \omega$, $A_3 = -\gamma_{m1}/2 + i\omega$, $A_4 = -\gamma_{m2}/2 + i\omega$. Based on the transmission probability of the probe field $T_{ij}(\omega)$ $(i, j = 1, 2)$, we can investigate the the optical nonreciprocal response in the four-mode optomechanical system.

3. The optical nonreciprocal response

In this section, we numerically evaluate the transmission probability of the probe field to prove the possibility of the optical nonreciprocal response in the four-mode optomechanical system. According to the numerical results, the optimum parameters for observing the optical nonreciprocal response are obtained. Relevant parameters are taken as $\kappa_{01} = \pi \times 10^6$ Hz, $\kappa_{02} = 2\pi \times 10^6$ Hz, $\kappa_{ex1} = \kappa_{ex2} = 4\pi \times 10^6$ Hz, $\gamma_{m3} = \gamma_{m4} = 4\pi \times 10^6$ Hz, $G_1 = 4\pi \times 10^6$ Hz, $G_2 = 6\pi \times 10^6$ Hz, $\theta = \pi/3$, $J = (2\kappa_1\kappa_2)^{1/2}$, $V = 0.1\gamma_{m3}$.[48]

In Fig. 2, we plot the transmission probability of the probe field $|T_{ij}|^2$ $(i, j = 1, 2)$ as a function of the $\omega/2\pi$ with $\phi = \pi/2$ (red dashed lines) and $\phi = -\pi/2$ (green solid lines), where the parameters are $\kappa_1 = 5\pi \times 10^6$ Hz, $\kappa_2 = 6\pi \times 10^6$ Hz, $\gamma_{m3} = \gamma_{m4} = 4\pi \times 10^6$ Hz, $G_1 = 4\pi \times 10^6$ Hz, $G_2 = 6\pi \times 10^6$ Hz, $\theta = \pi/3$, $J = (2\kappa_1\kappa_2)^{1/2}$, $V = 0.1\gamma_{m3}$. Under the condition of the phase difference $\phi = \pm\pi/2$, there are two peaks near the two frequencies with the probe detuning $\omega \simeq \pm 5\pi \times 10^6$ Hz and dip near the frequency with the probe detuning $\omega \simeq 0$ in the spectrum line of $|T_{ij}|^2$ $(i = j = 1, 2)$. At the same time, $|T_{12}|^2$ is always not equal to $|T_{21}|^2$ in the process of probe detuning ω from $-8\pi \times 10^6$ Hz to $8\pi \times 10^6$ Hz, that is to say, transmission probability of the probe field does not satisfy the Lorentz reciprocal theorem, and there appears the optical nonreciprocal response. When the phase difference $\phi = -\pi/2$, we have $|T_{12}|^2 < |T_{21}|^2$. When the phase difference $\phi = \pi/2$, we have $|T_{12}|^2 > |T_{21}|^2$. For example, when the phase difference $\phi = -\pi/2$, $|T_{21}|^2 \simeq 0.3$ while $|T_{12}|^2 = 0$ at $\omega = 0$. This shows that the probe field can be transmitted from cavity c_1 to cavity c_2, but the transmission from cavity c_2 to cavity c_1 is almost prohibited. The optical nonreciprocal response arises due to interference between two possible paths, where one path is along $c_1 \to b_3 \to c_2$ and the other path is along $c_1 \to c_2$. When $\phi = -\pi/2$, constructive interference between the two paths leads to the optical transmission from cavity c_1 to cavity c_2, but oppositely the optical transmission cavity c_2 to cavity c_1 is forbidden due to destructive interference.[48] The case of $\phi = \pi/2$ is exactly opposite to that of $\phi = -\pi/2$, $|T_{12}|^2 \simeq 0.3$ whereas $|T_{21}|^2 = 0$ at $\omega = 0$. Consequently, the optical nonreciprocal response can be realized based on the four-mode optomechanical system.

Figure 3 shows the transmission probability of the probe field $|T_{12}|^2$ (blue dashed line) and $|T_{21}|^2$ (red solid line) as a function of the phase difference ϕ/π. As shown in Fig. 3, the transmission probability of the probe field shows regular periodic oscillation. The $|T_{12}|^2 = |T_{21}|^2$ when $\omega = 0$ and $\phi = \pm n\pi$ (n is an integer). When $\phi \neq \pm n\pi$ (n is an integer), the $|T_{12}|^2 \neq |T_{21}|^2$, the time-reversal symmetry is broken, and the four-mode optomechanical system presents the optical nonreciprocal response. The optimal optical nonreciprocal response is obtained as $\phi = -\pi/2 \pm 2n\pi$ [$|T_{12}|^2 \simeq 0$ and $|T_{21}|^2 \simeq 0.3$] and $\phi = \pi/2 \pm 2n\pi$ [$|T_{12}|^2 \simeq 0.3$ and $|T_{21}|^2 \simeq 0$] (n is an integer).

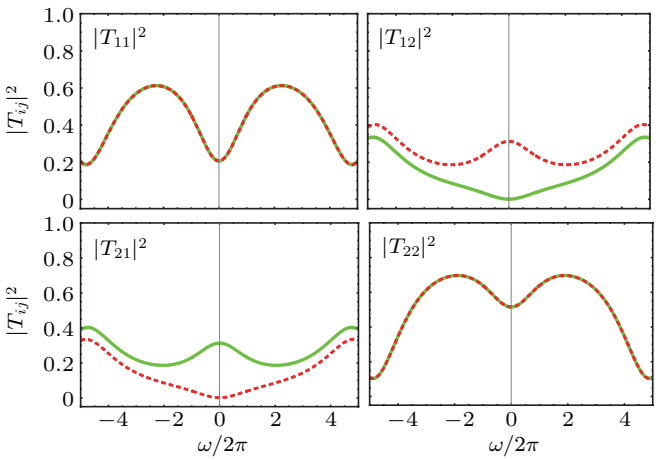

Fig. 2. The transmission probabilities $|T_{ij}|^2$ $(i, j = 1, 2)$ as a function of the $\omega/2\pi$. (i) The red dashed lines show the $\phi = \pi/2$, (ii) green solid lines show the $\phi = -\pi/2$. The values of the other parameters are set as $\kappa_{01} = \pi \times 10^6$ Hz, $\kappa_{02} = 2\pi \times 10^6$ Hz, $\kappa_{ex1} = \kappa_{ex2} = 4\pi \times 10^6$ Hz, $\gamma_{m3} = \gamma_{m4} = 4\pi \times 10^6$ Hz, $G_1 = 4\pi \times 10^6$ Hz, $G_2 = 6\pi \times 10^6$ Hz, $\theta = \pi/3$, $J = (2\kappa_1\kappa_2)^{1/2}$, $V = 0.1\gamma_{m1}$.

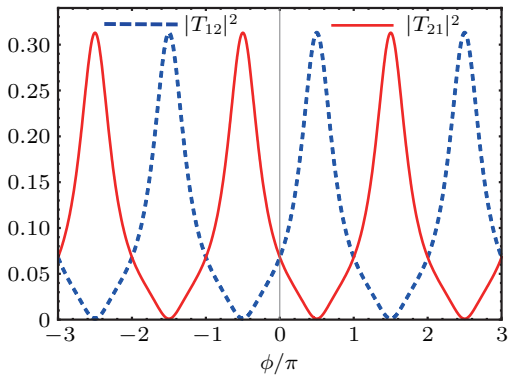

Fig. 3. The transmission probabilities $|T_{12}|^2$ (blue dashed line) and $|T_{21}|^2$ (red solid line) versus ϕ/π with $\omega = 0$. The other parameters are the same as those in Fig. 2.

The Coulomb interaction is also an important parameter. Therefore, the transmission probability of the probe field $|T_{12}|^2$ (blue dashed lines) and $|T_{21}|^2$ (red solid lines) plotted as a function of the $\omega/2\pi$ are shown in Fig. 4 for different Coulomb interaction at the phase $\phi = -\pi/2$: (a) $V = 0.1\gamma_{m3}$, (b) $V = 0.5\gamma_{m3}$, (c) $V = \gamma_{m3}$, (d) $V = 12\gamma_{m3}$. We can see that the Coulomb interaction has a significant influence on transmission probability of the probe field $|T_{12}|^2$ and $|T_{21}|^2$. When the Coulomb interaction is much smaller than the mechanical damping rate γ_{m3}, e.g., $V = 0.1\gamma_{m3}$ [see Fig. 4(a)], $|T_{12}|^2 \neq |T_{21}|^2$, and the optical nonreciprocal response is pronounced with the $\omega = 0$. However, as the Coulomb interaction

increases, the optical nonreciprocal response becomes invisible with the $\omega = 0$ [see Figs. 4(b) and 4(c)]. When $V = 12\gamma_{m3}$, $|T_{12}|^2$ is equal to and $|T_{21}|^2$, as shown in Fig. 4(d), the optical nonreciprocal response disappears. From Figs. 4(a)–4(d), we can see that the smaller the Coulomb interaction, the more obvious the optical nonreciprocal response. The optimal optical nonreciprocal response is obtained as $V = 0.1\gamma_{m3}$. From Eq. (1), we can obtain the steady-state mean value of mechanical mode b_3 as follows:

$$b_{s3} = \frac{-\mathrm{i}\left(g_1|c_{s1}|^2 + g_2|c_{s2}|^2\right)\cos\theta/2}{\gamma_{m3}/2 + \mathrm{i}\omega_{m3} + \frac{V^2}{\gamma_{m4}/2+\mathrm{i}\omega_{m4}}} = \frac{-\mathrm{i}\left(g_1|c_{s1}|^2 + g_2|c_{s2}|^2\right)\cos\theta/2}{\gamma'_{m3}/2 + \mathrm{i}\omega'_{m3}},$$

with

$$\gamma'_{m3}/2 = \gamma_{m3}/2 + \frac{V^2\gamma_{m4}/2}{(\gamma_{m4}/2)^2 + \omega_{m4}^2},$$

$$\omega'_{m3} = \omega_{m3} - \frac{V^2\omega_{m4}}{(\gamma_{m4}/2)^2 + \omega_{m4}^2},$$

where γ'_{m3} and ω'_{m3} are the effective damping and the effective detuning, c_{s1} and c_{s2} are the steady-state mean values of optical modes c_1 and c_2, respectively. Because of the existence of Coulomb interaction, the $\gamma_{m3}/2$ adds a term $\frac{V^2\gamma_{m4}/2}{(\gamma_{m4}/2)^2+\omega_{m4}^2}$. We can see that the γ'_{m3} increases with Coulomb interaction. The interaction between b_3 and other modes are decoupled with the increase of the effective damping. We also know that the optical nonreciprocal response arises due to interference between two possible paths, where one path is along $c_1 \to b_3 \to c_2$ and the other path is along $c_1 \to c_2$. Therefore, if the Coulomb interaction becomes larger, the interference effect between the two paths will become weaker. This is the reason why the optical nonreciprocal response gradually disappears when the Coulomb interaction is greatly enhanced.

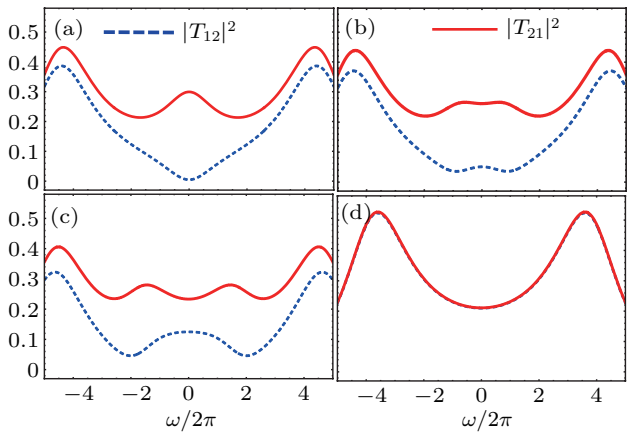

Fig. 4. The transmission probabilities $|T_{12}|^2$ (blue dashed lines) and $|T_{21}|^2$ (red solid lines) versus $\omega/2\pi$ with $\phi = -\pi/2$. (a) $V = 0.1\gamma_{m3}$, (b) $V = 0.5\gamma_{m3}$, (c) $V = \gamma_{m3}$, (d) $V = 12\gamma_{m3}$. The other parameters are the same as those in Fig. 2.

To further understand the effect of the Coulomb interaction on the transmission probability of the probe field, we plot the probability of the transmission $|T_{12}|^2$ (blue dashed line) and $|T_{21}|^2$ (red solid line) as a function of Coulomb interaction V/γ_{m3} in Fig. 5. We assume that the parameters $\phi = -\pi/2$, $\omega = 0$ and other parameters are the same as those in Fig. 2. It can be seen from Fig. 5 that $|T_{21}|^2$ is a decreasing function of V/γ_{m3}, whereas $|T_{12}|^2$ is opposite. It can be easily observed that the optical nonreciprocal response only exists in a limited value range of $V \leq 5\gamma_{m3}$. When the Coulomb interaction V is stronger than $5\gamma_{m3}$, the transmission probability from cavity c_2 to cavity c_1 is the same as the transmission probability from cavity c_1 to cavity c_2, $|T_{12}|^2 \approx |T_{21}|^2$. The values of $|T_{12}|^2$ and $|T_{21}|^2$ tend to be closer and closer to 0.21 as the Coulomb interaction is gradually increased, and the optical nonreciprocal response cannot be observed.

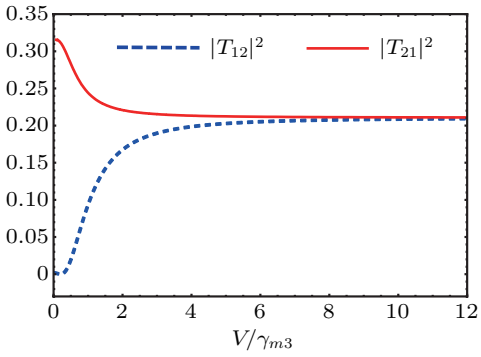

Fig. 5. The transmission probabilities $|T_{12}|^2$ (blue dashed line) and $|T_{21}|^2$ (red solid line) versus V/γ_{m3} with $\phi = -\pi/2$, $\omega = 0$. The other parameters are the same as those in Fig. 2.

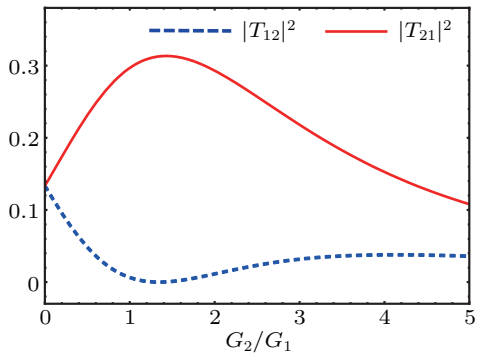

Fig. 6. The transmission probabilities $|T_{12}|^2$ (blue dashed line) and $|T_{21}|^2$ (red solid line) versus G_2/G_1 with $\phi = -\pi/2$, $\omega = 0$. The other parameters are the same as those in Fig. 2.

The effective optomechanical coupling strengths G_i $(i = 1,2)$ are also a critical parameters in the optomechanical system. Next, we discuss the effect of the effective optomechanical coupling strengths G_i $(i = 1,2)$ on the transmission probability of the probe field. The transmission probability of the probe field $|T_{12}|^2$ (blue dashed line) and $|T_{21}|^2$ (red solid line) plotted as a function of the G_2/G_1 are shown in Fig. 6. When $G_2/G_1 < 1.5$, $|T_{21}|^2$ increases with increasing G_2/G_1,

and $|T_{12}|^2$ is suppressed by the increasing G_2/G_1. By contrast, when $G_2/G_1 > 1.5$, with the further increase of G_2/G_1, $|T_{21}|^2$ gradually decreases and $|T_{12}|^2$ gradually increases. In the neighborhood of $G_2/G_1 = 1.5$, $|T_{21}|^2$ reaches the maximum $|T_{21}|^2 = 0.33$, $|T_{12}|^2$ reaches the minimum $|T_{12}|^2 = 0$, the optical nonreciprocal response is the most obvious. The results show that G_2/G_1 can influence the optical nonreciprocal response, which agrees with our theoretical prediction. The optimal optical nonreciprocal response is obtained as $G_2/G_1 = 1.5$.

4. Conclusions

In summary, we have investigated the optical nonreciprocal response in a four-mode optomechanical system. This system involves the Coulomb interaction and the optomechanical interaction. Under the condition of the strong coupling field, the phase difference between the optomechanical couplings, the Coulomb interaction, the effective optomechanical coupling strengths on the optical nonreciprocal response are analyzed. The results show that the optical nonreciprocal response is caused by the quantum interference between the optomechanical couplings and the linearly coupled interaction that breaks the time-reversal symmetry. In addition, we can obtain the optimum parameters for observing optical nonreciprocal response. We also see that the Coulomb effect has a negative effect on the optical nonreciprocal response.

References

[1] Yan X B 2017 *Phys. Rev. A* **96** 053831
[2] Agarwal G S and Huang S M 2010 *Phys. Rev. A* **81** 041803
[3] Weis S, Rivière R, Deleglise S, Gavartin E, Arcizet O, Schliesser A and Kippenberg T J 2010 *Science* **330** 1520
[4] Bai C, Hou B P, Lai D G and Wu D 2016 *Phys. Rev. A* **93** 043804
[5] Wei W Y, Yu Y F and Zhang Z M 2018 *Chin. Phys. B* **27** 034204
[6] Lu T X, Jiao Y F, Zhang H L, Saif F and Jing H 2019 *Phys. Rev. A* **100** 013813
[7] Lü H, Wang C Q, Yang L and Jing H 2018 *Phys. Rev. Appl.* **10** 014006
[8] Zhang H, Saif F, Jiao Y and Jing H 2018 *Opt. Express* **26** 25199
[9] Lü H, Jiang Y J, Wang Y Z and Jing H 2017 *Photon. Res.* **5** 367
[10] Jiao Y F, Lu T X and Jing H 2018 *Phys. Rev. A* **97** 013843
[11] Jiao Y, Lü H, Qian J, Li Y and Jing H 2016 *New J. Phys.* **18** 083034
[12] Jing H, Özdemir Sxahin K, Geng Z, Zhang J, Lü X Y, Peng B, Yang L and Nori F 2015 *Sci. Rep.* **5** 9663
[13] Yang Q, Hou B P and Lai D G 2017 *Opt. Express* **25** 9697
[14] Yan X B, Jia W Z, Li Yong, Wu J H, Li X L and Mu H W 2015 *Front. Phys.* **10** 351
[15] Guo Y J, Li K, Nie W J and Li Y 2014 *Phys. Rev. A* **90** 053841
[16] Liu Y M, Bai C H, Wang D Y, Wang T, Zheng M H, Wang H F, Zhu A D and Zhang S 2018 *Opt. Express* **26** 6143
[17] Liu Y C, Xiao Y F, Luan X S, Gong Q and Wong C W 2015 *Phys. Rev. A* **91** 033818
[18] Zhang S, Zhang J Q, Zhang J, Wu C W, Wu W and Chen P X 2014 *Opt. Express* **22** 28118
[19] Huang S M and Agarwal G S 2009 *Phys. Rev. A* **80** 033807
[20] Lü X Y, Jing H, Ma J Y and Wu Y 2015 *Phys. Rev. Lett.* **114** 253601
[21] Wu S C, Qin L G, Lu J and Wang Z Y 2019 *Chin. Phys. B* **28** 074204
[22] Wu Q 2016 *Chin. Phys. B* **25** 010304
[23] Cheng J, Liang X T, Zhang W Z and Duan X M 2018 *Chin. Phys. B* **27** 120302
[24] Zhang Y B, Liu J H, Yu Y F and Zhang Z M 2018 *Chin. Phys. B* **27** 074209
[25] Yan J K, Zhu X F and Chen B 2018 *Chin. Phys. B* **27** 074214
[26] Mu Q X, Lang C and Zhang W Z 2019 *Chin. Phys. B* **28** 114206
[27] Min F X, Xiao X Y, Yu Y F and Zhang Z M 2015 *Chin. Phys. B* **24** 050301
[28] Xia W Q, Yu Y F and Zhang Z M 2017 *Chin. Phys. B* **26** 054210
[29] Yan X B, Cui C L, Gu K H, Tian X D, Fu C B and Wu J H 2014 *Opt. Express* **22** 4886
[30] Yan X B, Deng Z J, Tian X D and Wu J H 2019 *Opt. Express* **27** 24393
[31] Yan X B, Fu C B, Gu K H, Wang R and Wu J H 2013 *Opt. Commun.* **308** 265
[32] Liu Y L, Wang C, Zhang J and Liu Y X 2018 *Chin. Phys. B* **27** 024204
[33] Ma P C, Zhang J Q, Xiao Y, Feng M and Zhang Z M 2014 *Phys. Rev. A* **90** 043825
[34] Zhang J Q, Li Y, Feng M and Xu Y 2012 *Phys. Rev. A* **86** 053806
[35] Wang J, Tian X D, Liu Y M, Cui C L and Wu J H 2018 *Laser Phys.* **28** 065202
[36] Wang Y P, Zhang Z C, Yu Y F and Zhang Z M 2019 *Chin. Phys. B* **28** 014202
[37] Bi L, Hu J, Jiang P, Kim D H, Dionne G F, Kimerling L C and Ross C A 2011 *Nat. Photon.* **5** 758
[38] Huang R, Miranowicz A, Liao J Q, Nori F and Jing H 2018 *Phys. Rev. Lett.* **121** 153601
[39] Chang L, Jiang X, Hua S, Yang C, Wen J, Jiang L, Li G, Wang G and Xiao M 2014 *Nat. Photon.* **8** 524
[40] Fang K, Yu Z and Fan S 2012 *Phys. Rev. Lett.* **108** 153901
[41] Wang D W, Zhou H T, Guo M J, Zhang J X, Evers J and Zhu S Y 2013 *Phys. Rev. Lett.* **110** 093901
[42] Korneeva Y P, Vodolazov D Y, Semenov A V, Florya I N, Simonov N, Baeva E, Korneev A A, Goltsman G N and Klapwijk T M 2018 *Phys. Rev. Appl.* **9** 064037
[43] Shen Z, Zhang Y L, Chen Y, Zou C L, Xiao Y F, Zou X B, Sun F W, Guo G C and Dong C H 2016 *Nat. Photon.* **10** 657
[44] Maayani S, Dahan R, Kligerman Y, Moses E, Hassan A U, Jing H, Nori F, Christodoulides D N and Carmon T 2018 *Nature* **558** 569
[45] Li B, Huang R, Xu X W, Miranowicz A and Jing H 2019 *Photon. Res.* **7** 630
[46] Li Y, Huang Y Y, Zhang X Z and Tian L 2017 *Opt. Express* **25** 018907
[47] Mirza I M, Ge W C and Jing H 2019 *Opt. Express* **27** 25515
[48] Jiang C, Song L N and Li Y 2018 *Phys. Rev. A* **97** 053812
[49] Jiang C, Baowei J I, Cui Y S, Zuo F, Shi J and Chen G 2018 *Opt. Express* **26** 15255
[50] Jiang C, Song L N and Li Y 2019 *Phys. Rev. A* **99** 023823
[51] Xu X W and Li Y 2015 *Phys. Rev. A* **91** 053854
[52] Xu X W, Li Y, Chen A X and Liu Y X 2016 *Phys. Rev. A* **93** 023827
[53] Xu X W, Song L N, Zheng Q, Wang Z H and Li Y 2018 *Phys. Rev. A* **98** 063845
[54] Yan X B, Lu H L, Gao F and Yang L 2019 *Front. Rhys.* **14** 52601
[55] Xia C C, Yan X B, Tian X D, Gao F 2019 *Opt. Commun.* **451** 197
[56] Zhang L W, Li X L and Yang L 2019 *Acta Phys. Sin.* **68** 170701 (in Chinese)
[57] Paternostro M, Gigan S, Kim M S, Blaser F and Böhm H R 2006 *New J. Phys.* **8** 107
[58] DeJesus E X and Kaufman C 1987 *Phys. Rev. A* **35** 5288